

UC Berkeley

UC Berkeley Previously Published Works

Title

On the relationship between stress and elastic strain for porous and fractured rock

Permalink

<https://escholarship.org/uc/item/7p83q5qj>

Journal

International Journal of Rock Mechanics & Mining Sciences, 46(2)

Author

Liu, Hui-Hai

Publication Date

2009

Peer reviewed



Contents lists available at ScienceDirect

International Journal of Rock Mechanics & Mining Sciences

journal homepage: www.elsevier.com/locate/ijrmms

On the relationship between stress and elastic strain for porous and fractured rock

Hui-Hai Liu*, Jonny Rutqvist, James G. Berryman

Earth Sciences Division, Lawrence Berkeley National Laboratory, Berkeley, CA 94720, USA

ARTICLE INFO

Article history:

Received 25 February 2008

Received in revised form

11 April 2008

Accepted 15 April 2008

Available online 22 May 2008

Keywords:

Stress–strain relationship

Hooke's law

Constitutive relationships

Nonlinearity

ABSTRACT

Modeling the mechanical deformations of porous and fractured rocks requires a stress–strain relationship. Experience with inherently heterogeneous earth materials suggests that different varieties of Hooke's law should be applied within regions of the rock having significantly different stress–strain behavior. We apply this idea by dividing a rock body conceptually into two distinct parts. The natural strain (volume change divided by rock volume at the current stress state), rather than the engineering strain (volume change divided by the unstressed rock volume), should be used in Hooke's law for accurate modeling of the elastic deformation of that part of the pore volume subject to a relatively large degree of relative deformation (i.e., cracks or fractures). This approach permits the derivation of constitutive relations between stress and a variety of mechanical and/or hydraulic rock properties. We show that the theoretical predictions of this method are generally consistent with empirical expressions (from field data) and also laboratory rock experimental data.

© 2008 Elsevier Ltd. All rights reserved.

1. Introduction

Mechanical deformation processes in porous and fractured rock and their coupling to thermal and hydrological processes are important for many applications [1], including geothermal energy development [2,3], oil and gas extraction [4], nuclear waste disposal [5,6], geological sequestration of carbon dioxide [7], and deep well injection of liquid and solid wastes [8,9]. With the significant advancement of computer technology in recent decades, numerical models have been increasingly employed for evaluating coupled mechanical, hydrological, and thermal processes associated with these applications [10].

The stress–strain relationship is fundamental for modeling mechanical deformation and the associated coupled processes in porous and fractured rock. Hooke's law has been generally used to describe this stress–strain relationship for elastic mechanical processes. Hooke's law, an approximation for small deformations, states that the amount by which a material (e.g., rock) body is deformed (the strain) is linearly related to the force (stress) causing the deformation. Nevertheless, the current application of the Hooke's law to porous and fractured rock is not without questions. Strictly speaking, the proportionality in the observed stress–strain relationship should be constant if the current application of Hooke's law is perfectly valid. However, it is not

unusual to see studies indicating that the proportionality is not always constant, but rather stress-dependent in many cases [11,12]. A number of efforts have been made to relate this stress-dependent behavior to the microstructures of “cracks” in porous rock [13–15]. An excellent review of these efforts is provided in a chapter entitled *Micromechanical Models* in Jaeger et al. [16]. Because it is generally difficult to characterize small-scale structures accurately and then relate their properties to large-scale mechanical properties that are of practical interest, it is desirable to have a macroscopic-scale theory that does not rely on the detailed description of small-scale structures, and that can physically incorporate the stress-dependent behavior of relevant mechanical properties. The first objective of this study is to develop a theory of this kind within the framework of Hooke's law.

For a stress-sensitive rock, the stress–strain relationship largely determines the relationships between stress and other rock mechanical/hydraulic properties, and these relationships control the degree of coupling between mechanical and hydrological processes [7,17]. However, the commonly used relationships between stress and hydraulic properties (such as porosity and fracture aperture) are generally empirical [7,18]. The second objective of this study is to derive mathematical formulations for these constitutive relationships based on our newly proposed stress–strain relationship.

This paper is organized as follows. We first present the development of a stress–strain relationship, and then derive constitutive relationships between stress and hydraulic/mechanic

* Corresponding author. Tel.: +1 510 486 6452; fax: +1 510 486 5686.
E-mail address: hhlui@lbl.gov (H.-H. Liu).

properties. Comparisons are then made between these relationships and the corresponding empirical expressions and experimental data, to test and evaluate the validity of our theoretical approach.

2. Theory

This section presents a new stress–strain relationship for porous and fractured rock based on Hooke's law. For simplicity, we mainly consider the relationship here for the volumetric strain, although our results can be easily extended to other types of strains.

Assume that a uniformly distributed force is imposed on the surface of a homogeneous and isotropic material body subject to elastic deformation. In this case, Hooke's law can be expressed as

$$d\sigma = K d\varepsilon_{v,t} \quad (1)$$

where σ is the hydrostatic stress (the compressive direction is positive), K is bulk modulus, and $\varepsilon_{v,t}$ is the natural or true volumetric strain defined by [19]

$$d\varepsilon_{v,t} = -\frac{dV}{V} \quad (2)$$

where V is the total volume of the material body under the current state of stress. In Eqs. (1) and (2), a decrease in the volume is considered to be positive. Our hypothesis herein is that Hooke's law holds for natural strains in some regions of a rock body. In the literature of material science, Freed [19] provided a historical review of the development of the concept of natural strain and argued that the natural strain should be used for accurately describing material deformation.

In previous studies [16], the following definition of strain (so-called engineering strain $\varepsilon_{v,e}$) is often used when applying Hooke's law:

$$d\varepsilon_{v,e} = -\frac{dV}{V_0} \quad (3)$$

where V_0 is the unstressed bulk volume. When the engineering strain is employed in Hooke's law, one can obtain the following relationship by integrating Eq. (3) and using the condition that $V = V_0$ for $\sigma = 0$:

$$V = V_0 \left(1 - \frac{\sigma}{K}\right) \quad (4)$$

Similarly, the use of natural strain in Hooke's law [Eq. (2)] yields

$$V = V_0 \exp\left(-\frac{\sigma}{K}\right) \quad (5)$$

It is easily seen that Eqs. (4) and (5) are nearly identical for small values of σ/K (or small strain).

In the literature of rock mechanics, the engineering strain has been exclusively used considering that the elastic strain is generally small. Porous and fractured rock, however, differs from purely solid materials in that it is inherently heterogeneous and includes both a solid phase and pores (and/or fractures) having a variety of geometric shapes. While the elastic strain is indeed small in most of the rock for stress changes of practical interest, the strain can be considerably larger within some portions of a rock body. For example, some pores (or fractures) in a rock can be subject to significant deformation, and even completely closed under a certain range of stress changes encountered in practice. For these pores, the strain is not small (on the order of one). An accurate description of the deformation of this portion of the rock is important for coupled mechanical and hydrological processes, because fluid flow occurs in pores and fractures.

To deal with this issue, we conceptualize the heterogeneous rock as having two parts, and hypothesize that one part (a portion

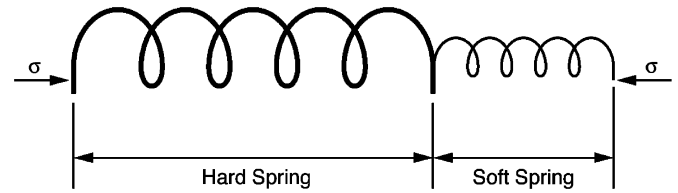


Fig. 1. A composite spring system consisting of two springs. The hard and soft springs follow engineering-strain-based and natural-strain-based Hooke's law, respectively.

of pore volume or fracture apertures) obeys a natural-strain-based Hooke's law, and the other part follows an engineering-strain-based Hooke's law. For simplicity, the first part is called "soft" part and the other called "hard" part. This conceptualization can be represented by a hypothesized composite spring system shown in Fig. 1. These two springs are subject to the same stress, but follow different varieties of Hooke's law. Berryman [20] also divided a poroelastic medium into "hard" and "soft" portions for the similar purpose in studying anisotropy of pore-fluid enhanced shear modulus. Mavko and Jizba [21] considered rock porosity to consist of a soft part and a stiff part in studying grain-scale fluid effects on velocity dispersion in rocks. Our "two-part" conceptualization is generally consistent with these previous studies. In this work, we use subscripts 0, e, and t to denote the unstressed state, the hard part (where engineering-strain-based Hooke's law applies) and the soft part (where natural (or true)-strain-based Hooke's law applies), respectively, for a rock body. Then we have

$$V_0 = V_{0,e} + V_{0,t} \quad (6)$$

and

$$dV = dV_e + dV_t \quad (7)$$

Applying Eqs. (4) and (5) to rock volumes V_e and V_t , respectively, in Eq. (7) yields

$$-\frac{dV}{V_0} = \gamma_e \frac{d\sigma}{K_e} + \gamma_t \exp\left(-\frac{\sigma}{K_t}\right) \frac{d\sigma}{K_t} \quad (8)$$

$$\gamma_t = \frac{V_{0,t}}{V_0} \quad (9)$$

$$\gamma_e = 1 - \gamma_t \quad (10)$$

where K_e and K_t refer to bulk moduli for the hard and soft parts, respectively. Eqs. (8)–(10) together comprise our proposed stress–strain relationship.

We should emphasize that our theory is a macroscopic-scale approximation that uses natural-strain-based Hooke's law to describe nonlinear deformation behavior of a fraction of pore volume (consisting of a collection of pores with a variety of geometry) subject to larger deformations. This nonlinear deformation could result from combining effects of non-uniform pore size distributions and pore geometry heterogeneity [16]. A rough fracture can also be considered a collection of pores with different sizes and geometries for the purpose of deformation calculations. The validity of this approximation will be evaluated in the following sections.

3. Constitutive relationships

In this section, we will use our newly developed stress–strain relationship to derive constitutive relationships between stress and mechanical/hydraulic properties for porous and fractured rock subject to elastic deformation. The derived relationships are

also compared with the corresponding empirical expressions and experimental data.

3.1. Bulk rock compressibility

Bulk rock compressibility characterizes the capability for a rock body to deform when stress is changed under a constant pore-pressure condition. Mathematically, the bulk rock compressibility is defined by [16]:

$$C_{bc} = -\frac{1}{V_0} \frac{\partial V}{\partial \sigma} \quad (11)$$

Substituting Eq. (8) into (11) yields

$$C_{bc} = \frac{\gamma_e}{K_e} + \frac{\gamma_t}{K_t} \exp\left(-\frac{\sigma}{K_t}\right) \quad (12)$$

This stress–compressibility relation consists of two terms. The first term is a constant; the second term is an exponential function. In fact, a number of researchers [12,16,22] have already noticed that rock compressibility data can often be empirically fitted to exponentially decreasing functions of the form:

$$C_{bc} = C_{bc}^\infty + (C_{bc}^i - C_{bc}^\infty) \exp\left(-\frac{\sigma}{P}\right) \quad (13)$$

where the superscript *i* denotes the initial (zero stress) value, the superscript ∞ denotes the value at high stress, and *P* is considered as a characteristic stress. Based on certain assumptions, Jaeger et al. [16] rewrote the above equation as

$$C_{bc} = C_{bc}^\infty + \frac{\phi_{crack}}{P} \exp\left(-\frac{\sigma}{P}\right) \quad (14)$$

where ϕ_{crack} refers to the porosity of crack-like voids in a porous rock sample. These voids were considered to be responsible for observed nonlinear deformation [16]. Zimmerman [12] fit measured compressibilities of three consolidated sandstones, Boise, Berea, and Bandera, to functions of the form of Eq. (13). We refer the readers to Zimmerman [12] for details of the curve-fitted results.

Several interesting observations can be made when comparing our result [Eq. (12)] with Eq. (13) or (14). First, the functional forms of Eqs. (12) and (14) are identical, indicating that our theoretical result is consistent with the corresponding empirical expressions and the related experimental data used to develop these expressions. Second, the curve-fitted results of Zimmerman [12] indicate that γ_t in Eq. (12) [or ϕ_{crack} in Eq. (14)] ranges from 0.2% to 0.5% for the three sandstones under consideration. It is much smaller than a typical porosity value for a sandstone rock (between 10% and 20%), suggesting that the so-called soft part of the rock body is only a small percentage of pore volume. This seems to be confirmed by the results to be discussed later in this paper. Third, values for K_t for the three sandstones (4.74–8.33 MPa) are significantly smaller (by three orders of magnitude) than those for K_e (9.5–12.2 GPa), indicating that the part where natural strain should be used is significantly “softer” than the rest of the rock body. This is consistent with our theoretical argument that different varieties of Hooke’s law should be used for different parts of porous and fractured rock. Note that the second term on the right hand side of Eq. (12) is not necessarily smaller than the first one, especially for low stress states, although γ_t is generally small, as demonstrated in Fig. 2.

A relationship between bulk compressibility and stress was also developed by Shapiro and his coworkers [23–25], based on an assumption that the compressibility is a linear function of crack porosity and change in the stiff porosity (that is similar to rock porosity of the hard part in this study). As indicated in Shapiro [23], their relationship is valid only for relatively small stress. Our

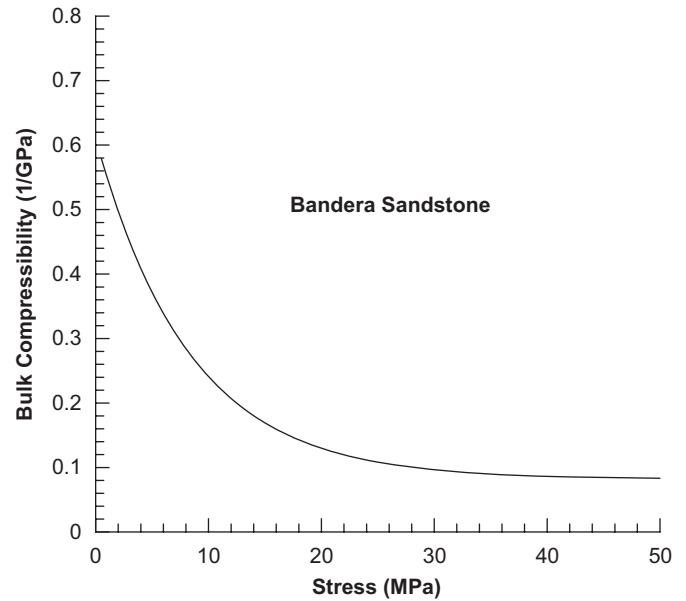


Fig. 2. Bulk compressibility as a function of stress calculated from Eq. (14) using the fitted parameter values ($C_{bc}^\infty = 0.082 \text{ GPa}^{-1}$, $P = 8.33 \text{ MPa}$ and $\phi_{crack} = 0.0044$) reported in [12].

Eq. (12) is different from their relationship in that there is an additional term (a linear function of stress) in their relationship. As discussed in MacBeth [26], several studies demonstrated that this additional term is not necessary for adequately fitting laboratory measurements and the inclusion of this term can make fitted parameter values unphysical in some cases. This supports the validity of our Eq. (12) that does not include this linear-functional term. It is important to note that our Eq. (12) is developed based on a rather general theoretical framework in which the soft part of the rock follows natural-strain-based Hooke’s law, which is fundamentally different from the approach presented by Shapiro [23].

3.2. Pore compressibility

The pore compressibility represents the change in pore volume per unit of stress change under a condition of constant pore pressure. Mathematically, this compressibility can be expressed by

$$C_{pc} = -\frac{1}{V_0^p} \frac{\partial V^p}{\partial \sigma} \quad (15)$$

where superscript *p* refers to pores. (The above equation holds for constant pore pressures.) Using similar notions from Section 2, we have

$$V_0^p = V_{0,e}^p + V_{0,t} \quad (16)$$

$$V^p = V_e^p + V_t \quad (17)$$

Note that in the above two equations, we consider V_t to be a portion of pore volume in a rock body. Following the same procedure used to derive Eqs. (3) and (4), we obtain

$$dV_e^p = -C_e V_{0,e}^p d\sigma \quad (18)$$

$$dV_t = -\frac{V_{0,t}}{K_t} \exp\left(-\frac{\sigma}{K_t}\right) d\sigma \quad (19)$$

where C_e is the compressibility for the hard fraction of pore volume where engineering strain is applicable. This treatment is based on our argument that all the soft part corresponds to some fraction of pore volume.

Combining Eqs. (15)–(19) yields

$$C_{pc} = C_{pc}^\infty + \frac{\gamma_t}{\phi_0 K_t} \exp\left(-\frac{\sigma}{K_t}\right) \quad (20)$$

where

$$C_{pc}^\infty = C_e \frac{V_{0,e}^p}{V_0^p} \quad (21)$$

$$\phi_0 = \frac{V_0^p}{V_0} \quad (22)$$

Eq. (20) is used to fit one set of compressibility data (Fig. 3) presented in Jaeger et al. [16]. This data set was derived from a measured relationship between pore strain and confining stress for a Frio sandstone from East Texas (after Carpenter and Spencer [27]). The match between Eq. (20) and the data points is satisfactory, indicating that our derived result is able to capture the key features of these experimental observations. The fitted parameter values are: $C_{pc}^\infty = 3.33 \times 10^{-6} \text{ psi}^{-1} = 4.83 \times 10^{-4} \text{ MPa}^{-1}$, $K_t = 1.1 \times 10^3 \text{ psi} = 7.6 \text{ MPa}$, and $\gamma_t/\phi_0 = 0.011$. For typical porosity (ϕ_0) values of 10–20% for a sandstone, the γ_t value from pore compressibility data ranges from 0.11% to 0.22%, which again suggests that the so-called “soft” part is only a small percentage of pore volume. These parameter values are reasonably close to those obtained from rock compressibility data provided in the previous subsection.

3.3. Rock porosity

The rock porosity (ϕ) is a critical parameter for fluid flow in porous rock. Accurate descriptions of stress-dependent behavior for porosity are especially important for modeling coupled hydrological and mechanical processes. In this subsection, we derive a theoretical relationship between rock porosity and stress.

Using the same notations as in the previous subsection and by definition of rock porosity, we have

$$d\phi = \frac{dV^p}{V} = \frac{dV_e^p + dV_t}{V} \quad (23)$$

where V is the bulk volume of porous rock. (Note that the above equation ignores the effect of the change in V with stress on the porosity change. An expression for $d\phi$ that does not make this assumption is given on p. 38 of [12].) If we approximate V by the unstressed volume V_0 for calculating rock porosity, then using this approximation and Eqs. (18) and (19), we obtain

$$d\phi = -\phi_e C_e d\sigma - \frac{\gamma_t}{K_t} \exp\left(-\frac{\sigma}{K_t}\right) d\sigma \quad (24)$$

where

$$\phi_e = \phi_0 - \gamma_t \quad (25)$$

Integrating Eq. (24) and using $\phi = \phi_0$ for $\sigma = 0$ gives

$$\phi = \phi_e(1 - C_e\sigma) + \gamma_t \exp\left(-\frac{\sigma}{K_t}\right) \quad (26)$$

When the term $C_e\sigma$ is much smaller than unity, the above equation can be approximately reduced to

$$\phi = \phi_e + \gamma_t \exp\left(-\frac{\sigma}{K_t}\right) \quad (27)$$

Based on laboratory experiments on sandstone by Davis and Davis [28], Rutqvist et al. [7] proposed an empirical stress-porosity expression that is identical in form to Eq. (27). Similar empirical expressions were originally reported by Athy [29] and further discussed in Neuzil [18]. In this work, the more general stress-porosity relation [Eq. (26)] is evaluated using data sets of Coyner [30]. He reported measured porosity–confining pressure (effective stress) relations for several types of rock. We select his laboratory measurements for Berea sandstone and Weber sandstone samples, because these rock samples exhibit a relatively large degree of stress dependence. Note that confining pressure is used here to approximate the effective stress, since Biot coefficients are close to unity for the two sandstones under consideration [17].

There are four parameters in Eq. (26): ϕ_e , C_e , γ_t and K_t . To avoid as much as possible the non-uniqueness of parameter values

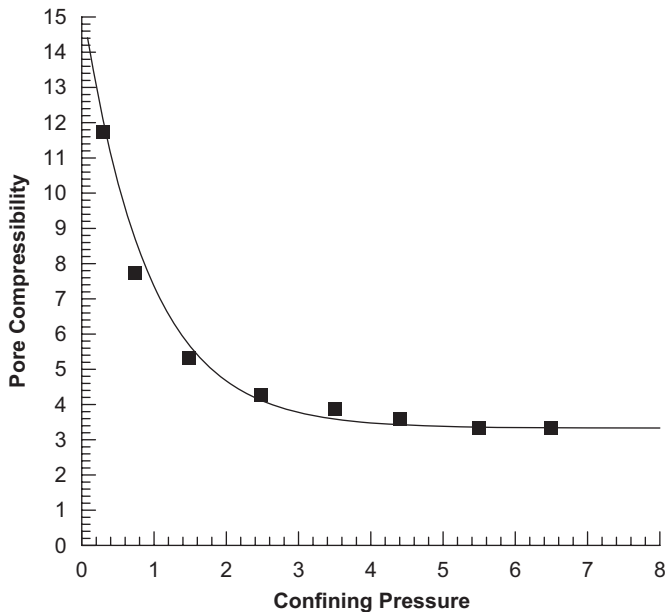


Fig. 3. Match of Eq. (20) to the data points of pore compressibility (10^{-6} psi^{-1}) as a function of confining pressure (or stress) (psi) presented in [16].

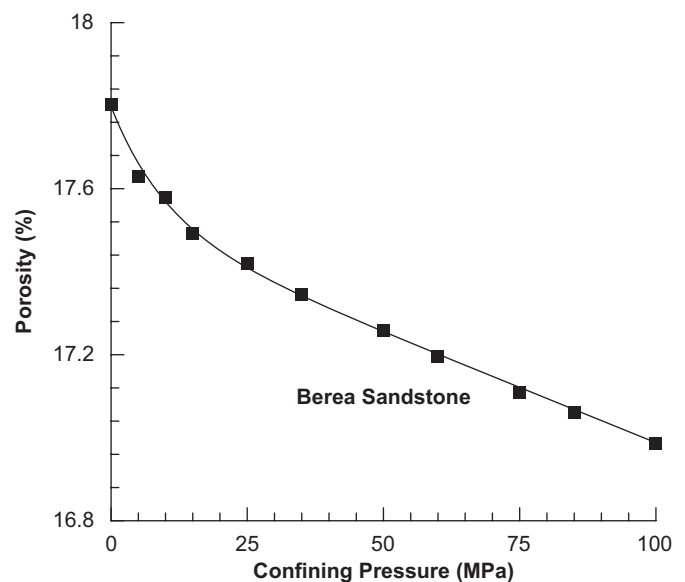


Fig. 4. Match between porosity values (as a function of confining pressure) calculated from Eq. (26) and the measured data for Berea sandstone [30].

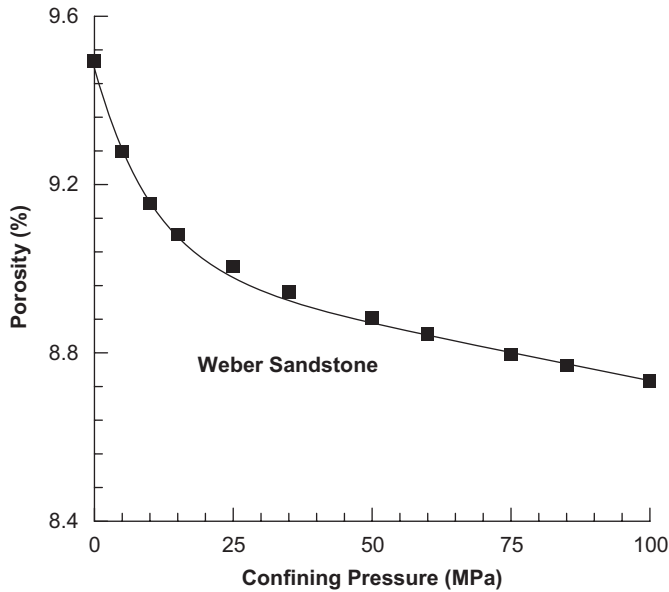


Fig. 5. Match between porosity values (as a function of confining pressure) calculated from Eq. (26) and the measured data for Weber sandstone [30].

determined from curve fitting, we use a simple procedure to estimate parameter values from porosity vs. confining pressure data. As shown in Figs. 4 and 5, measured relations between porosity and confining pressure are very well represented by a straight line for relatively high pressures (stresses). The slope of the straight line is used to determine $\phi_e C_e$ because the second term on the right hand side of Eq. (26) is negligible for high stress values. The porosity value at the intersection between the straight line and the vertical axis in Fig. 4 or 5 gives ϕ_e value, considering that the straight line represents the first term on the right hand side of Eq. (26). The measured porosity value at zero pressure is equal to $\phi_e + \gamma_t$, as implied from Eq. (26). The above procedure allows for direct determination of values for ϕ_e , C_e , and γ_t . The remaining parameter K_t can be estimated using porosity data at relatively low pressures. In this study, the chosen K_t value is simply calculated from Eq. (26), using measured porosity value at a pressure of 10 MPa.

Satisfactory matches between results calculated from Eq. (26) (with determined parameter values) and porosity data are shown in Figs. 4 and 5. The estimated parameter values for Berea sandstone are $\phi_e = 17.52\%$, $C_e = 3.04 \times 10^{-4} (\text{MPa}^{-1})$, $\gamma_t = 0.28\%$ and $K_t = 9.97 \text{ MPa}$. The parameter values for Weber sandstone are $\phi_e = 9.00\%$, $C_e = 2.96 \times 10^{-4} (\text{MPa}^{-1})$, $\gamma_t = 0.48\%$ and $K_t = 10.60 \text{ MPa}$. These parameter values are also presented in Table 1. Note that the values for γ_t and K_t are generally consistent with those reported in the previous sections where the values for these parameters are estimated from different types of data. This indicates that these two parameters (introduced in this study) are very well defined and experimentally robust.

To further validate our theory, we use parameter values estimated from porosity data to calculate relations between the bulk modulus and pressure (stress) and check if the calculated results can match the measured bulk modulus data for the same rock samples used for measuring porosity values [30]. From our stress–strain relationship [Eq. (8)], the bulk modulus K is given by

$$K = \frac{1}{(\gamma_e/K_e) + (\gamma_t/K_t) \exp(-\sigma/K_t)} \quad (28)$$

The above equation can also be derived from Eq. (12). Values for K_e/γ_e correspond to K values for high stresses (pressures) and must

Table 1
Fitted parameter values from the experiment data of Coyner [30]

Sandstones	ϕ_e (%)	C_e (MPa^{-1})	γ_t (%)	K_t (MPa)
Berea	17.52	3.04×10^{-4}	0.28	9.97
Weber	9.00	2.96×10^{-4}	0.48	10.60

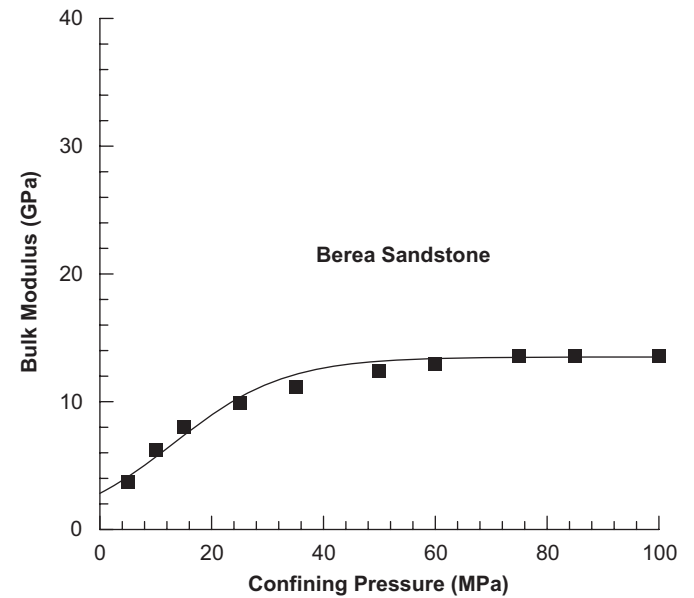


Fig. 6. A comparison between bulk modulus values (as a function of confining pressure) calculated from Eq. (26) and the measured data for Berea sandstone [30].

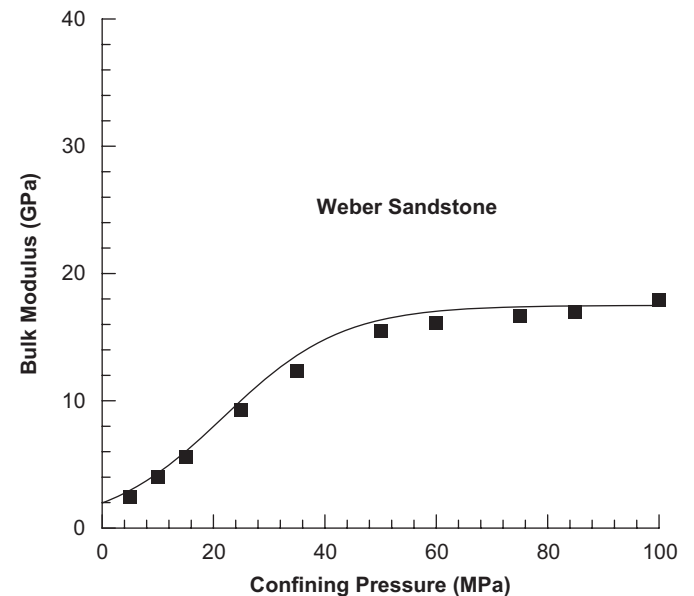


Fig. 7. A comparison between bulk modulus values (as a function of confining pressure) calculated from Eq. (26) and the measured data for Weber sandstone [30].

be determined from measured K data. (They cannot be determined from porosity data.) Based on data shown in Figs. 6 and 7, the value of K_e/γ_e is set to 13.5 GPa for Berea sandstone and 17.5 GPa for Weber sandstone. As shown in Figs. 6 and 7, the calculated results are in a good agreement with data. This is encouraging (considering that a curve-fitting procedure is not

used in these two figures) and also supports the robustness of our theory.

MacBeth [26] proposed a formula to describe the sensitivity of the bulk modulus for a sandstone rock framework under applied isotropic loading, by assuming (1) that the rock frame’s stress dependence arises from a distribution of small-scale flaws or elements of compliance [31,32] and (2) that the dependence of compliance on stress is an exponential function of stress. His formula for the bulk modulus is essentially the same as our Eq. (28), and was successfully used to fit 179 sets of laboratory measurements on unsaturated reservoir core and outcrop sandstones that have low to moderate porosity and a range of clay fractions and cementation. This again supports the validity of our Eq. (28), and thereby also substantially extends the set of rocks to which the method has been successfully applied.

3.4. Fracture aperture

Fracture aperture is an important parameter for both mechanical and hydraulic processes within a fractured rock. For example, fracture permeability is largely determined by fracture aperture. A number of empirical expressions exist in the literature for describing observed relations between normal stress and fracture closure (that is linearly related to the average fracture aperture) [33,34]. In this subsection, we develop a relationship for the dependence of fracture aperture on the normal stress based on the proposed stress–strain relationship.

Consider a fracture to be embedded into a rock sample subject to a normal stress σ_n . We again divide fracture space into “hard” and “soft” parts along the direction normal to the fracture plane. Then, the volumetrically averaged fracture aperture (b) is given by

$$b_0 = b_{0,e} + b_{0,t} \tag{29}$$

under unstressed conditions, and

$$b = b_e + b_t \tag{30}$$

under stressed conditions. Similar to previous sections, subscripts e and t (for “engineering” and “true,” respectively) refer to the “hard” and “soft” parts in a fracture. Hooke’s law for the two parts can be expressed by

$$d\sigma_n = -K_{F,e} \frac{db_e}{b_{0,e}} \tag{31}$$

$$d\sigma_n = -K_{F,t} \frac{db_t}{b_t} \tag{32}$$

where subscript F refers to fracture. (For convenience, the volumetric strain will not be used here.) Note that the stress in the above two equations refers to far-field normal stress, rather than local stress.

Combining Eqs. (30)–(32) gives

$$db = db_e + db_t = -b_{0,e} \frac{d\sigma_n}{K_{F,e}} - b_t \frac{d\sigma_n}{K_{F,t}} \tag{33}$$

Integrating the above equation and using Eq. (29) and the following relationship obtained from Eq. (32):

$$b_t = b_{0,t} \exp\left(-\frac{\sigma_n}{K_{F,t}}\right) \tag{34}$$

one can obtain

$$b = b_{0,e} \left(1 - \frac{\sigma_n}{K_{F,e}}\right) + b_{0,t} \exp\left(-\frac{\sigma_n}{K_{F,t}}\right) \tag{35}$$

In the above equation, the stress-dependent behavior of fracture aperture is controlled by the second term at low stress and the

first term at high stress. Because $K_{F,e}$ is much larger than $K_{F,t}$, aperture change with stress will be much more gradual at high stress. This result is consistent with the observations of [35], that the increase of fracture closure (or decreasing of fracture aperture) with increasing normal stress becomes more gradual, but does not reach zero, and even at much higher stresses, a number of voids remain open. Nevertheless, there is a considerable amount of laboratory data indicating that fracture closure (or fracture aperture) remains practically unchanged at high stress [33,34]. This is equivalent to saying that the following condition holds in practice:

$$1 - \frac{\sigma_n}{K_{F,e}} \approx 1 \tag{36}$$

In this case, we can reduce Eq. (35) to

$$b = b_{0,e} + b_{0,t} \exp\left(-\frac{\sigma_n}{K_{F,t}}\right). \tag{37}$$

This equation is identical to the empirical expressions of [7] and [36] for the stress–fracture aperture relationship. The expression has been used successfully to match laboratory measurements. For example, Fig. 8 shows the match of Eq. (37) to the measurements of the third loading–unloading cycle for a fracture [37]. Some hysteresis has been observed. Barton et al. [34] suggested that the hysteresis was a laboratory artifact and that *in situ* fractures probably also behave in a manner similar to that observed from the third or fourth loading cycles.

The consistency of our Eq. (36) with the empirical expression of Rutqvist et al. [7] is encouraging. Fig. 8 shows that unlike the “soft” part of porous rock, the “soft” part in a fracture corresponds to a relatively large portion of fracture voids. This may result from a geometric difference between fractures and rock pores. Previous studies [38] demonstrate that a rock “crack” with a smaller aspect ratio (ratio of thickness to length) is more easily deformed than that with a smaller ratio. Obviously, values for the ratio are much larger for fractures than those for more equant pores in porous rock. Fig. 8 also shows the modulus for the fracture ($K_{F,t}$) is in the range of 2–4 MPa, and smaller than the previously reported

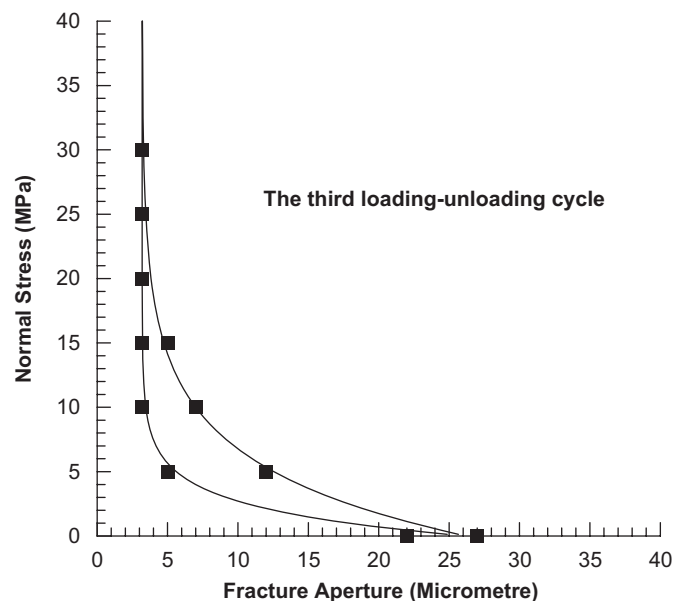


Fig. 8. Matches of Eq. (36) to the observed stress–aperture data points for a fracture in a volcanoclastic rock (Borrowdale Volcanic Group). The fitted parameter values are $b_{0,e} = 3 \mu\text{m}$, $b_{0,t} = 23 \mu\text{m}$, and $K_{F,t} = 3.3$ and 2.2 MPa, respectively, for the loading and unloading data points.

modulus values for the soft part of the porous rock. This is consistent with an intuitive expectation that a fracture is “softer” than are the non-fracture-like pores in rock.

The nonlinear nature of our aperture-stress relationship [Eq. (35)] is also consistent with nonlinear behavior in observed compressional and shear velocity data (as a function of stress) in fractured rocks [39]. This is because these velocities are closely related to fracture mechanical and geometry properties including aperture (or thickness of cracks), as discussed in [40]. Our Eq. (35) is developed for a single fracture, while a model using an elastic modulus tensor [32,41] may be needed for dealing with large-scale fracture aperture-stress relationships.

4. Concluding remarks

This work has developed a general stress–strain relationship for porous and fractured rock subject to elastic mechanical deformation, based on the hypothesis that different varieties of Hooke’s law need to be employed for different parts of a rock body, for describing the elastic mechanical deformation. The stress–strain relationship developed here is very general, including both linear and nonlinear components, and allows for the derivation of constitutive relationships between stress and a number of mechanical/hydraulic properties. The remarkable consistency between these relationships and a variety of the corresponding empirical expressions and/or laboratory experimental data tends to support the validity of our theoretical development. The parameter values estimated from different kinds of measurements are also close for similar rocks, indicating that newly introduced parameters are well defined and robust for the applications considered.

The focus of this paper has been on the presentation of a relatively simple and intuitive theoretical framework. Our preliminary evaluation produced encouraging results. Further work is still needed to validate our theory using more comprehensive comparisons between our results and those of different types of mechanical data. Also, it is both desirable and of practical interest to explore possible correlations among parameters characterizing the soft part of a rock, rock type, and the other associated rock properties. Important examples of related properties are electrical resistivity/conductivity data for fluid-saturated porous rocks [42–44] and also permeability data [45].

Acknowledgments

We are indebted to Seiji Nakagawa at Lawrence Berkeley National Laboratory for his critical and careful review of a preliminary version of this manuscript. Helpful comments of two referees are also gratefully acknowledged. This work was supported by the US Department of Energy (DOE), under DOE Contract no. DE-AC02-05CH11231.

References

- [1] Rutqvist J, Stephansson O. The role of hydromechanical coupling in fractured rock engineering. *Hydrogeol J* 2003;11:7–40.
- [2] Pine RJ, Batchelor AS. Downward migration of shearing in jointed rock during hydraulic injections. *Int J Rock Mech Min Sci* 1984;21:249–63.
- [3] Baria R, Baumgartner J, Rummel F, Pine RJ, Sato Y. HDR/HWR reservoirs: concepts, understanding and creation. *Geothermics* 1999;28:533–52.
- [4] Lewis RW, Schrefler BA. The finite element method in the static and dynamic deformation and consolidation of porous media. 2nd ed. New York: Wiley; 1998.
- [5] Tsang C-F. Introduction to coupled processes. In: Tsang CF, editor. *Coupled processes associated with nuclear waste repositories*. Orlando: Academic Press; 1987. p. 1–8.
- [6] Rutqvist J, Tsang C-F. Analysis of thermal-hydrologic-mechanical behavior near an emplacement drift at Yucca Mountain. *J Contam Hydrol* 2003;62–63:637–52.
- [7] Rutqvist J, Wu Y-S, Tsang C-F, Bodvarsson G. A modeling approach for analysis of coupled multiphase fluid flow, heat transfer, and deformation in fractured porous rock. *Int J Rock Mech Min Sci* 2002;39:429–42.
- [8] Apps J, Tsang C-F. Preface. In: Apps J, Tsang C-F, editors. *Deep injection of disposal of hazardous industrial waste: scientific and engineering aspects*. San Diego: Academic Press; 1996.
- [9] Brasier FM, Kobelsky BJ. Injection of industrial wastes in the United States. In: Apps J, Tsang C-F, editors. *Deep injection of disposal of hazardous industrial waste: scientific and engineering aspects*. San Diego: Academic Press; 1996. p. 1–8.
- [10] Jing L, Hudson JA. Numerical methods in rock mechanics. *Int J Rock Mech Min Sci* 2002;39:409–27.
- [11] Mavko G, Nur A. Melt squirt in the asthenosphere. *J Geophys Res* 1978;80:1444–8.
- [12] Zimmerman RW. *Compressibility of sandstones*. Amsterdam: Elsevier; 1991.
- [13] Walsh JB. The effect of cracks on the compressibility of rock. *J Geophys Res* 1965;70:381–9.
- [14] Walsh JB. The effect of cracks on the uniaxial elastic compression of rocks. *J Geophys Res* 1965;70:399–411.
- [15] Nur A. Effects of stress on velocity anisotropy in rocks with cracks. *J Geophys Res* 1971;76:2022–34.
- [16] Jaeger JC, Cook NGW, Zimmerman RW. *Fundamentals of rock mechanics*. 4th ed. Oxford: Blackwell; 2007.
- [17] Berryman JG. Effective stress for transport properties of inhomogeneous porous rock. *J Geophys Res* 1992;97(B12):17409–24.
- [18] Neuzil CE. Hydromechanical coupling in geologic processes. *Hydrogeol J* 2003;11:41–83.
- [19] Freed AD. Natural strain. *J Eng Mater Technol* 1995;117:379–85.
- [20] Berryman JG. Estimates and rigorous bounds on pore-fluid enhanced shear modulus in poroelastic media with hard and soft anisotropy. *Int J Damage Mech* 2006;15(2):133–67.
- [21] Mavko G, Jizba D. Estimating grain-scale fluid effects on velocity dispersion in rocks. *Geophysics* 1991;56:1940–9.
- [22] Wyble DO. Effect of applied pressure on the conductivity, porosity, and permeability of sandstones. *Petrol Trans AIME* 1958;213:430–2.
- [23] Shapiro SA. Piezosensitivity of porous and fractured rocks. *Geophysics* 2003;68:482–6.
- [24] Shapiro SA, Kaselow A. Porosity and elastic anisotropy of rocks under tectonic stress and pore pressure changes. *Geophysics* 2005;70:N27–38.
- [25] Becker K, Shapiro SA, Stanchits S, Dresen G, Vinciguerra S. Stress induced elastic anisotropy of the Etnean basalt: theoretical and laboratory examination. *Geophys Res Lett* 2007;34:L11307.
- [26] MacBeth C. A classification for the pressure-sensitivity properties of a sandstone rock frame. *Geophysics* 2004;69:497–510.
- [27] Carpenter CB, Spencer GB. Measurement of compressibility of consolidated oil-bearing sandstones. Report 3540. Denver: US Bureau of Mines, 1940.
- [28] Davis JP, Davis DK. Stress-dependent permeability: characterization and modeling. Society of Petroleum Engineers, paper SPE 56813, 1999.
- [29] Athy LF. Density, porosity, and compaction of sedimentary rock. *Am Assoc Petrol Geol Bull* 1930;14:1–24.
- [30] Coyner KB. Effects of stress, pore pressure, and pore fluids on bulk strain, velocity, and permeability of rocks. Ph.D. thesis, Massachusetts Institute of Technology, Cambridge, MA, 1984.
- [31] Sayers CM, Kachanov M. Microcrack-induced elastic wave anisotropy of brittle rocks. *J Geophys Res* 1995;100:4149–56.
- [32] Schoenberg M, Sayers CM. Seismic anisotropy of fractured rock. *Geophysics* 1995;60:204–11.
- [33] Goodman RE. *Methods of geological engineering in discontinuous rocks*. New York: West Publishing; 1976.
- [34] Barton NR, Bandis SC, Bakhtar K. Strength, deformation, and conductivity coupling of rock joint deformation. *Int J Rock Mech Min Sci* 1985;22:121–40.
- [35] Pyrak-Nolte LJ, Myer LR, Cook NGW, Witherspoon PA. Hydraulic and mechanical properties of natural fractures in low permeability. In: *Proceedings of the 6th international congress on rock mechanics*, Montreal. Rotterdam: Balkema, 1987. p. 225–31.
- [36] Daley TM, Schoenberg MA, Rutqvist J, Nihei KT. Fractured reservoir: an analysis of coupled elastodynamic and permeability changes from pore-pressure variation. *Geophysics* 2006;71:033–41.
- [37] Liu HH, Rutqvist J, Zhou Q, Bodvarsson GS. Upscaling of Normal stress-permeability relationships for fracture networks obeying the fractional Levy motion. In: Stephansson O, Hudson JA, Jing L, editors. *Coupled thermo-hydro-mechanical-chemical processes in geo-systems*. Amsterdam: Elsevier; 2004. p. 263–7.
- [38] Kachanov M. Elastic solids with many cracks and related problems. *Adv Appl Mech* 1994;30:259–445.
- [39] Stekly RM. Compressional and shear velocities of dry and saturated jointed rock: a laboratory study. *Geophys J R Astron Soc* 1985;83:239–62.

- [40] Hudson JA. Wave speeds and attenuation of elastic waves in material containing cracks. *Geophys J R Astron Soc* 1981;64:133–50.
- [41] Schoenberg M. Elastic wave behavior across linear slip interfaces. *J Acoust Soc Am* 1980;68:1516–21.
- [42] Brace WF, Orange AS, Madden TR. The effect of pressure on the electrical resistivity of water-saturated crystalline rocks. *J Geophys Res* 1965;70:5669–78.
- [43] Brace WF, Orange AS. Electrical resistivity in saturated rock under stress. *Science* 1966;153:1525–6.
- [44] Brace WF, Orange AS. Further studies of the effects of pressure on electrical resistivity of rocks. *J Geophys Res* 1968;73:5407–19.
- [45] Brace WF, Walsh JB, Frangos WT. Permeability of granite under high pressure. *J Geophys Res* 1968;73:2225–36.